Scaling Properties of Gold Nanocluster Chemiresistor Sensors

Mario G. Ancona, Arthur W. Snow, Edward E. Foos, Walter Kruppa, *Senior Member, IEEE*, and Robert Bass

Abstract—The effect of geometric scaling on the performance of metal-insulator metal-ensemble (MIME) chemiresistors based on gold nanoclusters is investigated. The ultrasmall size of the nanoclusters is shown to enable extreme scaling of the sensors with reductions in area of at least a factor of 10^4 over conventional MIME devices. If the operating voltage is held constant, the absolute sensitivity of the devices is found to remain essentially unchanged by the geometric scaling. Interestingly, this occurs despite the fact that contact resistance appears to play a significant role in the smallest devices. The detection limit of the sensors is set by a signal-to-noise ratio, and because $1/f$ noise tends to dominate, reduction in sensor size raises the noise floor, leading to a degradation in the detection limit. Because of the importance of the $1/f$ noise, optimal performance will be obtained by operating the sensors under ac conditions with filtering. Despite the degradation in performance that results from scaling, nanocluster-based chemiresistors of reduced size can still be advantageous because of the possibility of achieving vapor-sensing systems of substantially reduced size, power, complexity, and cost, as well as new applications, e.g., for sensor arrays.

Index Terms—Chemical-vapor sensing, chemiresistor, nanoclusters, scaling, $1/f$ noise.

I. INTRODUCTION

IN THE burgeoning field of nanoscience/nanotechnology, it has become popular to consider chemical sensing as an early application for whatever nanoscale material is currently of interest, whether it be a nanocluster, a nanotube, or a conducting molecule. This nanoscale-sensing work has potential for high performance because of the enhanced surface-to-volume ratios and the possibility of new transduction mechanisms, and indeed, some intriguing results have been obtained even down to the few-molecule regime [1], [2]. From a practical standpoint, however, these nanoscale sensors are currently problematic because of substantial obstacles associated with sampling, nonuniformity, nonlinear response (especially with multicomponent vapors), and noise. For these reasons, a more successful near-term strategy for exploiting advances in nanoscience is to devise chemical sensors that benefit from nanostructural features yet avoid the difficulties of nanofabrication and small-number statistics by incorporating large numbers of nanoscale

elements. This approach can be described as one based on nanostructured materials. One recent example of this is the "nanotube-mat" sensors devised by several groups [3]–[6] as a way of exploiting the transduction properties of carbon nanotubes in a reproducible fashion. An earlier example was the metal-insulator-metal-ensemble (MIME) sensors invented by Snow and Wohltjen that utilize the chemiresistance of metal-insulator-metal tunnel junctions in films of coated metallic nanoclusters [7]–[10]. One aspect of the latter approach not previously studied in detail is its tremendous potential for scalability that arises from its nanostructural character. This is the subject of this paper where we demonstrate that MIME sensors are indeed highly scalable with reductions in overall size easily made from the millimeter (or larger) scale of current technology to as small as 10 μm in linear dimension.

The chemiresistor concept has its origins in studies of photosynthesis, of the olfactory mechanism, and of conductive filler-insulating matrix composites. Simply defined, a chemiresistor is a device whose electrical resistance is changed by the presence of an interacting chemical species [11]. The device incorporates a thin film of a semiconducting material deposited onto a pair of contacting electrodes. The "semiconducting" material (i.e., a material with conductivity intermediate between a metal and an insulator) behaves as a transducer by converting the adsorption/absorption of a molecular species into an electronic signal. Features that govern the sensitivity of these devices are 1) the vapor pressure of the analyte; 2) the chemical interaction between the analyte vapor and the adsorbent surface's chemical structure; 3) the chemical and physical properties of the semiconducting material; and 4) the device design. In this paper, the focus is on the last factor and, particularly, on the effect geometric scaling has on the performance of chemiresistors in which a thin film of gold nanoclusters forms the semiconducting/transducing material [7]–[9].

Chemiresistor transduction materials generally divide into two types; those of an intrinsic semiconductor nature and those based on conducting particulate fillers loaded into an insulating matrix near the percolation threshold. The former involve a primary or secondary doping (electron transfer) interaction with an analyte vapor to modulate the number and/or mobility of the charge carriers. Examples dating back to the 1960s include substituted acetylene polymers [12], β-carotene [13], and phthalocyanine compounds [14]. While much research has been done [15]–[20], these sensors have technical problems (stability, reproducibility, selectivity, etc.), and none have been successfully commercialized. The second type of transduction material utilizes physical absorption of the analyte in the insulating matrix and a conductance change based on alteration

Report Documentation Page		Form Approved OMB No. 0704-0188

Public reporting burden for the collection of information is estimated to average 1 hour per response, including the time for reviewing instructions, searching existing data sources, gathering and maintaining the data needed, and completing and reviewing the collection of information. Send comments regarding this burden estimate or any other aspect of this collection of information, including suggestions for reducing this burden, to Washington Headquarters Services, Directorate for Information Operations and Reports, 1215 Jefferson Davis Highway, Suite 1204, Arlington VA 22202-4302. Respondents should be aware that notwithstanding any other provision of law, no person shall be subject to a penalty for failing to comply with a collection of information if it does not display a currently valid OMB control number.

1. REPORT DATE **APR 2006**	2. REPORT TYPE	3. DATES COVERED **00-00-2006 to 00-00-2006**
4. TITLE AND SUBTITLE **Scaling Properties of Gold Nanocluster Chemiresistor Sensors**		5a. CONTRACT NUMBER
		5b. GRANT NUMBER
		5c. PROGRAM ELEMENT NUMBER
6. AUTHOR(S)		5d. PROJECT NUMBER
		5e. TASK NUMBER
		5f. WORK UNIT NUMBER
7. PERFORMING ORGANIZATION NAME(S) AND ADDRESS(ES) **Naval Research Laboratory,4555 Overlook Avenue SW,Washington,DC,20375**		8. PERFORMING ORGANIZATION REPORT NUMBER
9. SPONSORING/MONITORING AGENCY NAME(S) AND ADDRESS(ES)		10. SPONSOR/MONITOR'S ACRONYM(S)
		11. SPONSOR/MONITOR'S REPORT NUMBER(S)

12. DISTRIBUTION/AVAILABILITY STATEMENT
Approved for public release; distribution unlimited

13. SUPPLEMENTARY NOTES

14. ABSTRACT

The effect of geometric scaling on the performance of metal-insulator metal-ensemble (MIME) chemiresistors based on gold nanoclusters is investigated. The ultrasmall size of the nanoclusters is shown to enable extreme scaling of the sensors with reductions in area of at least a factor of 104 over conventional MIME devices. If the operating voltage is held constant, the absolute sensitivity of the devices is found to remain essentially unchanged by the geometric scaling. Interestingly, this occurs despite the fact that contact resistance appears to play a significant role in the smallest devices. The detection limit of the sensors is set by a signal-to-noise ratio, and because 1/f noise tends to dominate, reduction in sensor size raises the noise floor, leading to a degradation in the detection limit. Because of the importance of the 1/f noise, optimal performance will be obtained by operating the sensors under ac conditions with filtering. Despite the degradation in performance that results fromscaling, nanocluster-based chemiresistors of reduced size can still be advantageous because of the possibility of achieving vapor-sensing systems of substantially reduced size, power, complexity, and cost, as well as new applications e.g., for sensor arrays.

15. SUBJECT TERMS

16. SECURITY CLASSIFICATION OF:			17. LIMITATION OF ABSTRACT	18. NUMBER OF PAGES	19a. NAME OF RESPONSIBLE PERSON
a. REPORT **unclassified**	b. ABSTRACT **unclassified**	c. THIS PAGE **unclassified**	**Same as Report (SAR)**	**12**	

of the connections between conducting particulates in the insulating matrix. These sensors have been called "adsistors" and one such sensor known as the "Adsistor Cold Sensor" was patented and commercialized in 1962 for gasoline leaks around boat engines [21]. More recent work on adsistors has used composites based on micrometer-size conductive fillers (vanadium oxide or carbon black) loaded into thermoplastic polymer matrices [polyethylene, poly(vinyl alcohol), poly(vinyl chloride), etc.] and relies on vapor-induced swelling of the polymer matrix [22]–[25]. These systems are more reproducible and stable and are better understood than those based on organic semiconductors. A commercialized version of the carbon-black polymer-composite 32-element sensor array has been marketed as Cyranose 320 by Smiths Detection [26]. The adsistors based on gold nanoclusters investigated in this paper owe their performance to the exponential sensitivity of the intercluster tunneling on the intercluster distance and barrier height. The modulation of these parameters by adsorbed vapors—in the simplest case, via swelling—gives the sensor sensitivity. The particular responses for a given cluster ligand shells produce selectivity (especially when an array of sensors is deployed) [7]–[9]. These nanocluster sensors can be expected to have the advantages of the adsistor type of sensor plus considerably greater scalability by virtue of the ultrasmall particulates.

To obtain a chemiresistive response out of a material that changes its electron-transport characteristics upon chemical exposure, there must be enough material present so that it can be characterized by macroscopic parameters such as electrical resistivity, partition coefficients, etc. In other words, a chemiresistor must contain enough discrete elements of the active material, e.g., polymer molecules or carbon particles, which the fluctuations associated with the underlying discreteness are negligible.[1] Thus, we require

$$\text{Size of sensor} \gg \begin{array}{c}\text{Size of discrete}\\\text{elements that form the}\\\text{chemiresistive material.}\end{array} \quad (1)$$

With regard to scaling, a crucial implication of this continuum assumption is that in order to obtain the smallest possible chemiresistor, one should have the smallest possible discrete elements that still exhibit the basic chemical-vapor sensitivity. Therefore, for instance, one can expect MIME sensors (with particle sizes of about 2 nm) to be much more scalable than carbon-particle adsistors (with particle sizes of about 1 μm). In scaling chemiresistors, one other factor that enters an understanding of their behavior is the possibility of contact effects—both contact resistance and contact chemiresistance—whose relative importance will obviously increase as the size is reduced. In this regard, MIME sensors would also seem attractive since the electron-transport mechanism between electrode and cluster is the same as the one between clusters (i.e., gold-to-gold tunneling), and so, one might expect that the contact contribution will be small. This contrasts with sensors based, for example, on a semiconducting polymer where Schottky contact effects are common and often dominate.

To understand the chemiresistor sensitivity and its scaling characteristics one needs to consider the contributions of both electrode-design and of the semiconductor material itself. In order to deconvolve the latter (at least partially as we shall see), one can normalize the measured current change associated with the vapor response to the baseline current measured under vapor-purged conditions. Most semiconducting-material studies have followed this practice and, in the process, lose information about the sensitivity and performance of the chemiresistor that is delivered by the design. Previous reports of scaling of the chemiresistor-electrode configurations that used this approach include: lead phthalocyanine on coplanar gold electrodes with a gap range of 5 to 100 μm [27]; poly(pyrrole) and poly(aniline) on gold parallel electrodes with a gap range of 11 to 55 μm [28]; and carbon-black–polyacrylate composite on gold ring and dot electrodes with a gap range of 10 to 500 μm [29]. In each case, the sensor response is expressed as a fractional change relative to the baseline and is found to be independent of the electrode gap. In other words, the intrinsic transduction capacity of the material is unaffected by the geometry. Nevertheless, the overall sensitivity of the chemiresistor is impacted by geometry since the measured signal is current (not normalized current). For this reason, this paper considers the vapor response both in raw form as well as normalized. Furthermore, since the basic measure of performance is a signal-to-noise ratio, our scaling study needs to be concerned with both the signal and the noise. Because our interest is in chemiresistors operating with known applied voltage, the signal is the change in current per given amount of vapor (i.e., the "current sensitivity"), while the noise is a current noise. Regarding the latter, in this paper, we keep things simple by considering only noise associated with the resistance itself and ignore any possible additional contributions that arise from the vapor exposure. The nanocluster material is composed of 1.7-nm gold nanoclusters deposited as a film onto interdigitated and coplanar electrodes with electrode gaps ranging from 0.1 to 25 μm and electrode widths varying from 25 μm to 48 cm. As noted, we generally keep the voltage constant no matter the size of the device. Although a constant electric-field scaling scenario (i.e., with average electric field held constant in the scaling) might seem more appropriate since the maximum biasing that can be applied to a given device will presumably be set by some maximum electric field $E_{\max}$ above which nonlinear or irreversible effects start to become significant, the matter turns out to be unimportant because, as we shall find in Section V, above some relatively low electric-field value, the sensor performance becomes essentially independent of the voltage. Lastly, our interest is primarily in the response to changes in vapor concentration ("concentration sensitivity"), and we only touch briefly on the separate question of response to the amount of vapor ("number sensitivity").

Finally, it is worthwhile to note that the main payoff in being able to scale the nanocluster-based chemiresistor technology is that smaller chemiresistors and chemiresistor arrays will enable sensor-system scaling that can in turn deliver substantial savings in system size, power, and cost, e.g., for drop-off or

---

[1]It is also important that the molecular discreteness of the chemical vapor itself be unimportant; this is usually the case given the density and time scales involved.
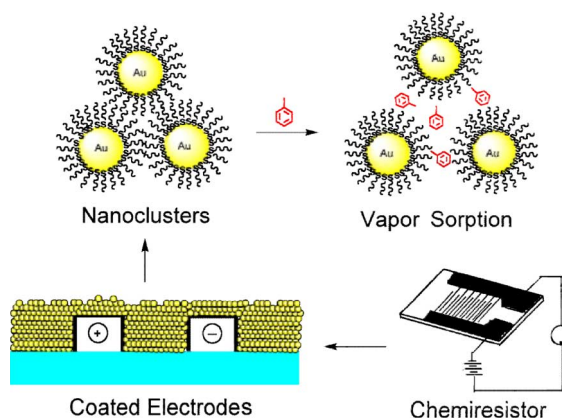
Fig. 1.   Schematic of MIME vapor sensor and its mechanism of operation.

wireless applications. It is also possible that the small sizes will allow new kinds of chemiresistor applications to be developed.

II. MIME-Chemiresistor Fabrication

Introduced in 1998 [7]–[9], MIME chemiresistors are composed of films of metallic nanoclusters whose electrical resistance is modulated by the adsorption of chemical vapors (see Fig. 1). As noted in Section I, MIME sensors are a type of adsistor that employs very small particle sizes. The metallic cores of the individual particles are typically only 1–5 nm in diameter, composed of gold, and encapsulated by a monolayer shell of organic molecules attached via gold-thiol chemistry. The clusters are synthesized by a modification of Brust's method [30] that allows the core and shell dimensions to be varied independently [7]–[9], [31]. In the original Brust synthesis, the cluster shell was formed of dodecanethiols. However, numerous other thiol-terminated molecules have since been studied in order to increase the chemical sensitivity and selectivity by enhancing the partitioning of particular vapors into the cluster film [31], [32]. The clusters studied in this paper have cores that are approximately 1.7 nm in diameter and with a shell composed of hexanethiolate molecules. The extremely small particle spacings in MIME sensors and the associated tunneling mechanism have been found experimentally to enhance sensitivity over other adsistors (with the same electrode geometry) from levels of parts-per-thousand with micrometer-scale particles [25] to parts-per-million [7]–[9]. In addition, the nanometer scale of the particles and their correspondingly large surface area translate into a dynamic-sensitivity range covering four or more orders in magnitude depending on the vapor. Finally, the loose packing of the nanoclusters is such that vapor molecules rapidly diffuse in and out through the nanoscale voids in the matrix of clusters resulting in extremely fast sensor response times.

The first step in making MIME sensors is fabricating the electroded substrate. In this paper, a number of electrode designs of varying geometry are employed to investigate the scalability of MIME sensors. Representative schematics and micrographs are shown in Fig. 2(a)–(d). The sensor in Fig. 2(a) is a conventional design with micrometer-scale interdigitated electrodes fabricated using optical lithography on a quartz or Si/SiO$_2$ substrate. In these devices, there are 50 fingers on each electrode with the spacing between the fingers ranging from
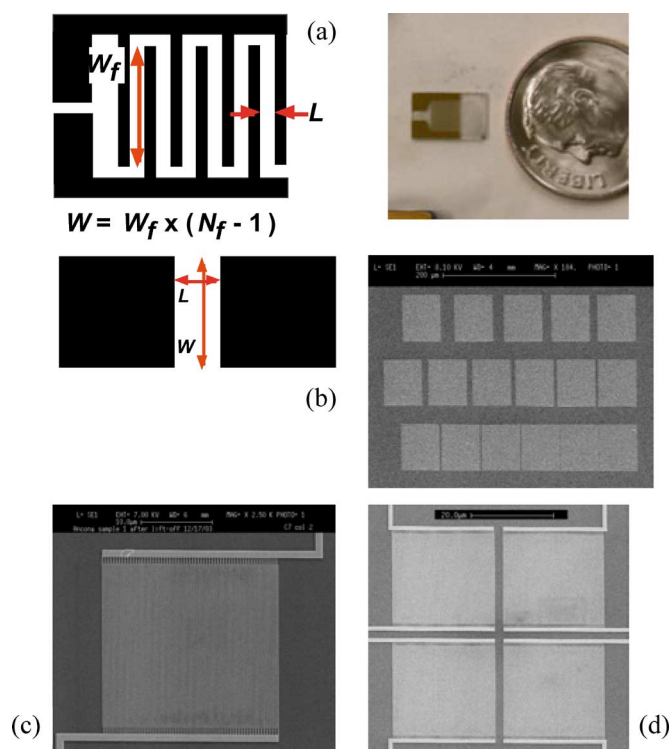

Fig. 2.   Electrode schematics and micrographs of various sensor test devices used in this paper. (a) Micrograph of a state-of-the-art MIME device (electrode gap = 2 μm). (b) Micrograph of large (90 mm) square pads with variables gaps. (c) SEM image of a scaled-MIME device (electrode gap = 130 nm). (d) SEM image of an array of four scaled-MIME devices.

$L = 2$ to 15 μm. The finger length W_f is 4800 μm so that the effective width W ($= W_f \times 99$ finger gaps) of the device is about 48 cm, and the entire device typically occupies over 10 mm^2 of area. The second group of test devices, which is shown in Fig. 2(b), is configured as an array of square electrodes that are separated by gaps of $L = 1$ to 25 μm and a fixed width of $W = 90$ μm. This array provides a finer coverage of device sizes, although because of their relatively small width, the larger gap devices show a significant amount of fringing current. The third type of sensor tested in this paper is shown in the SEM image in Fig. 2(c). It is simply a scaled version of the conventional interdigitated-electrode device of Fig. 2(a) with a near-identical W/L of around 32 000 and with SEM-measured finger gaps of $L = 0.123, 0.215,$ and 0.248 μm. These electrodes have been patterned using ordinary electron-beam lithography; a cheaper alternative, which is not explored in this paper but that would be more effective in a production environment, is nanoimprint lithography [33]. Finally, in Fig. 2(d), we illustrate the possibility of arrays formed of the highly scaled devices. The particular array shown contains four sensors, each of which has finger-gap dimensions of about $L = 0.1$ μm for a total area of only 0.0025 mm^2. A similar array created in conventional MIME technology would consume an area of close to 100 mm^2.

The second step in the sensor fabrication is to deposit the nanoclusters on the electroded substrates. For this paper, we employ an airbrush technique with substrate heating to speed the solvent evaporation. Although precise control of the thickness of such films is difficult, especially from batch to

batch, we estimate the film thickness in our films to be roughly 0.2-μm thick [7]–[9]. It is conceivable that this thickness could depend on the electrode geometry especially as the gaps get very narrow, e.g., as a result of shadowing. Other techniques for cluster deposition that have also been used are chemical self-assembly based on thiol exchange [34] and microcontact printing [35]. Although not directly relevant to this paper, if one wished to fabricate sensor arrays, then there would be the additional problem of functionalizing different sensor elements with different cluster formulations. When the sensors are far apart, this is relatively straightforward, but a closely spaced array like that in Fig. 2(d) would be quite challenging. In practice, one would undoubtedly have to increase the spacing between the sensors and then employ a shadow mask, microcontact printing, or perhaps a more sophisticated technique like that of [36].

III. SCALING ANALYSIS OF CHEMIRESISTORS

Before discussing the experimental results, it is useful to analyze the characteristics and scaling properties that one would expect for chemiresistors. This provides a basis for understanding and assessing the potential benefits of scaling, and it establishes a clear framework for interpreting experimental measurements and for evaluating the performance of actual sensors. The general analysis should apply at any temperature, although of course, the parameters characterizing the film will depend on temperature.

Prior to exposure to a chemical vapor, one can expect chemiresistive films satisfying the criterion in (1) to display ohmic current–voltage (I–V) characteristics, so long as the applied voltage is not too high. In other words, the current will obey Ohm's Law, $V = IR$, where R is a constant resistance. This resistance is composed of contributions from the film and from the two electrode contacts, which, being in series, are additive. For the electrode patterns displayed in Fig. 2 and the deposition technique described in Section II, it seems reasonable to assume that the nanocluster film is macroscopically homogeneous, and that the electron transport is essentially one dimensional (1-D). In this case, the film and contact resistances can be expressed in terms of the bulk conductivity of the film σ_f (in Siemens per micron) and the interfacial conductivity σ_c (in square Siemens per micron) of the contact so that we have

$$R = \frac{L}{W d \sigma_\mathrm{f}} + \frac{2}{W d \sigma_\mathrm{c}} \qquad (2)$$

where d is the average film thickness, and the factor of two accounts for the two contacts that are presumed identical. It should be noted that when the electrodes are interdigitated [as in the devices shown in Fig. 2(a) and (c)], W is the equivalent width of a parallel plate design.

When a voltage V is applied across the electrodes, a current $I = V/R$ will be measured. If the device is then exposed to a chemical vapor, a change in current $\Delta I = V \Delta(1/R)$, due to the vapor-induced changes in the film and contact resistances, will be observed. Since it is the change in current that is measured, we characterize the **sensitivity** of the chemiresistor by

the size of the current change induced by a given concentration of analyte. Thus, we define

$$\text{Chemiresistor sensitivity}: \qquad \Sigma_a \equiv \frac{\partial I}{\partial c_a} \qquad (3)$$

where c_a is the concentration of analyte a in the ambient air or in a preconcentrated air stream. This sensitivity is usually (although not always) reasonably constant over a broad range of concentrations. To relate the sensitivity of the chemiresistor to the vapor-induced changes in the film conductivity σ_f (in Siemens per micron) and the contact conductivity σ_c (in square Siemens per micron), we define intrinsic sensitivities of the film and contact

$$r_a^\mathrm{f} \equiv \frac{\partial \sigma_\mathrm{f}}{\partial c_a^\mathrm{f}} \qquad r_a^\mathrm{c} \equiv \frac{\partial \sigma_\mathrm{c}}{\partial c_a^\mathrm{c}} \qquad (4)$$

where c_a^f and c_a^c are the concentrations of analyte a in the film and contacts, respectively. For a given chemiresistor, these intrinsic sensitivities can be expected to be essentially constant as long as the chemiresistive film and contacts are not close to saturation, and there are not strong interaction effects between multiple analytes. Furthermore, at low-analyte concentration, the amount of analyte in the film and the contact will be linearly related to the analyte concentration in the sensor's headspace, i.e.,

$$c_a^\mathrm{f} = k_a^\mathrm{f} c_a \quad \text{and} \quad c_a^\mathrm{c} = k_a^\mathrm{c} c_a \qquad (5)$$

where k_a^f and k_a^c are the partition coefficients for the analyte a in the film and contact regions, respectively. For simplicity, we shall assume that $k_a^\mathrm{f} = k_a^\mathrm{c} \equiv k_a$. It should be noted that the relationships in (5) are for equilibrium and do not allow for chemical kinetic effects.

The change in current that would result from exposure to analyte a is given by

$$\Delta I = \frac{\partial I}{\partial c_a} \Delta c_a = V \frac{\partial (1/R)}{\partial c_a} \Delta c_a$$

and using (2)–(5), we obtain the following expression for the chemiresistor sensitivity:

$$\Sigma_a \equiv \frac{\partial I}{\partial c_a} = \frac{V W d}{L} k_a r_a^\mathrm{f} \frac{1 + \beta r}{(1 + \beta)^2}$$

$$\text{where} \quad \beta \equiv \frac{2 \sigma_\mathrm{f}}{\sigma_\mathrm{c} L} \quad \text{and} \quad r \equiv \frac{r_a^\mathrm{c} \sigma_\mathrm{f}}{r_a^\mathrm{f} \sigma_\mathrm{c}}. \qquad (6)$$

The quantity β is a dimensionless parameter that measures the relative importance of the bulk and contact conductivities, and r is the dimensionless ratio of the relative intrinsic sensitivities of the contacts and the film. The contribution of the contact

chemiresistance will be "small" when $\beta \ll 1$, and r is not too large, and in this case, (6) reduces to

$$\Sigma_a \cong \frac{k_a V W d r_a^{\mathrm{f}}}{L}. \tag{7}$$

According to this formula, we can obtain higher sensitivity by: 1) improving the intrinsic sensitivity r_a^{f}; 2) enhancing the partitioning of vapor into the film k_a; 3) modifying the geometry to increase Wd/L; and/or 4) raising the voltage V. If d, W/L, and V are held fixed during scaling, then (7) indicates that the absolute sensitivity will be unaffected by geometric scaling.

Because the transduction effected by a chemiresistor involves the conversion of a chemical concentration to an electric current, the absolute-sensitivity parameter Σ_a defined above is usually the appropriate measure of sensitivity. As it should, this definition implies that a sensor with a higher absolute sensitivity will yield a bigger current signal for a given amount of analyte, and if the noise floor stays the same, this translates into a lower detection limit. However, once the vapor-induced current change has been measured, it can be more useful for purposes of interpretation to work with the normalized or relative current change (i.e., $\Delta I/I$, where I is the baseline current) rather than the measured absolute current change itself. The justification for this statement is readily deduced from (6)

$$\frac{\Delta I}{I} = \frac{1}{I}\frac{\partial I}{\partial c_a}\Delta c_a = \frac{\Sigma_a}{I}\Delta c_a = \frac{k_a r_a^{\mathrm{f}}}{\sigma_{\mathrm{f}}}\left[\frac{1+\beta r}{1+\beta}\right]\Delta c_a \tag{8}$$

which, when contact effects are neglected, reduces to

$$\frac{\Delta I}{I} = \frac{k_a r_a^{\mathrm{f}}}{\sigma_{\mathrm{f}}}\Delta c_a. \tag{9}$$

The advantage of using the relative current change is evident from these formulas and especially from (9). For large devices, (9) will be appropriate, and it says that the relative current change (unlike the absolute current change) will be independent of geometrical effects and of voltage or electric field. This makes it a more reliable measure of the response, e.g., if one wishes to enhance selectivity by a chemometric analysis of the outputs from an array of nominally identical sensors. From a chemistry standpoint, the relative current change is also useful because it provides a direct assessment of the contribution of the intrinsic film characteristics to the overall sensitivity Σ_a. When the sensor size is reduced, the relative current change is still useful, but as (8) shows, contact effects can give rise to a complicating dependence on geometry (through the parameter β) and particularly on the gap distance L. This could lead to problems in interpretation since one cannot then discriminate between a contact effect and a length-dependent change in the intrinsic film characteristics. It should be noted that this ambiguity disappears if the relative intrinsic sensitivities of the film and the contacts are roughly the same ($r \cong 1$). Finally, we remark that (as noted in the Introduction) some investigators have employed a relative sensitivity defined by Σ_a/I to evaluate sensor performance [27]–[29]. This relative sensitivity is less useful as a device engineering figure of merit because

it fails to account for the effects of geometry and voltage on performance.

Although the concentration sensitivity Σ_a is ordinarily of most relevance, in some cases, one is more interested in a chemiresistor's transduction of the number or mass of molecules (rather than their concentration) into an electrical current. In this situation, the appropriate measure of transduction efficiency is the number sensitivity, i.e., the size of the response induced by a change in the number of analyte molecules in the cluster film N_a^{f}. Using (6) and (7), and noting that $N_a^{\mathrm{f}} = c_a^{\mathrm{f}}WLd$, we can write

$$\Sigma_a^{\mathrm{num}} = \frac{\partial I}{\partial N_a^{\mathrm{f}}} = \frac{\Sigma_a}{k_a W L d} = \frac{V r_a^{\mathrm{f}}}{L^2}\left[\frac{1+\beta r}{(1+\beta)^2}\right] \cong \frac{V r_a^{\mathrm{f}}}{L^2} \tag{10}$$

where the rightmost approximation results when contact effects are neglected. The main implication of this formula is that the number sensitivity of the chemiresistor is benefited by a scaling of the electrode gap L (in either the constant voltage or constant field scaling scenarios) but not by a reduction in the device width W.

As noted in the Introduction, the performance of a sensor is set not just by the sensitivity of its transduction but also by how small a current change ΔI can be detected. This is of course determined by the noise floor, which in general has many contributions, not all of which are well understood. For simplicity in this paper, we assume the noise floor to be dominated by the noise arising from the resistance itself, and that other sources associated with the vapor exposure, with the transduction and with the measurement system, can be neglected. In future work, we hope to examine these other sources more closely with appropriate experiments and simulation.

Regarding the zero-vapor noise in a chemiresistor, it can be assumed that the behavior will be qualitatively like that of a typical resistor in being dominated by thermal noise and, at low frequencies, by "excess" $1/f$ or flicker noise, with shot noise being negligible because of the effect of long-range correlations [37]–[39]. Noise is generally characterized by its spectral density, and because we operate the sensors under an applied voltage with the current being measured, it is the current-noise spectral density that is of most interest here. The thermal current-noise spectral density is given by the well-known formula

$$S_{\mathrm{I}}^{\mathrm{thermal}} = \frac{4k_{\mathrm{B}}T}{R} \tag{11}$$

where k_{B} is Boltzmann's constant, and T is the temperature. Since the thermal noise scales with the resistance R, it should remain unchanged by any geometric scaling that keeps W/L fixed. The scaling behavior of the $1/f$ current noise is less certain, but an expectation can be derived from the Hooge formula

$$S_{\mathrm{I}}^{\mathrm{flicker}} = \frac{\alpha_{\mathrm{H}}I^2}{fN} \tag{12}$$

where N is the number of conducting electrons in the film, f is frequency, and α_{H} is the phenomenological Hooge

parameter [40]. Obviously, $1/f$ noise increases as the frequency is reduced. Two forms derived from (12) are

$$S_{\mathrm{I}}^{\mathrm{flicker}} = \frac{\alpha_{\mathrm{H}} V^2}{R^2 f N} = \frac{\alpha_{\mathrm{H}} V^2 \sigma_{\mathrm{f}}^2 d}{f n L^2 (1+\beta)^2} \frac{W}{L} \tag{13a}$$

$$\frac{S_{\mathrm{I}}^{\mathrm{flicker}}}{I^2} = \frac{\alpha_{\mathrm{H}}}{f N} = \frac{\alpha_{\mathrm{H}}}{f n L^2 d} \frac{L}{W} \tag{13b}$$

where $N \equiv nWLd$ defines n as the density of conducting electrons in the film. Although (12) and (13) assume dc biasing (V) so that I is the dc current, an analogous formula can be used under ac conditions since the $1/f$ noise is fundamentally associated with resistance fluctuations and since the induced current/voltage fluctuations are small compared to the amplitude of the applied ac bias. In this case, I and V should be replaced by their rms values.

Because thermal and $1/f$ noises are the primary intrinsic noise contributions, a useful concept is the idea of the corner frequency at which these two sources are equal. From (11) and (12), it is evident that $f_{\mathrm{corner}} = \alpha_{\mathrm{H}} IV/(4N k_{\mathrm{B}} T)$. Because the corner frequency is typically larger than the RC cutoff frequency f_{RC}, the operating frequency is usually below the corner frequency, and $1/f$ noise generally dominates. When this happens, (13a) shows that the noise will increase as the chemiresistor size decreases (assuming d, W/L, and V are held fixed), saturating as contact resistance comes to dominate (i.e., as the β term grows).

A final "noise" source that should be mentioned is baseline drift that is associated with "aging" effects and that is frequently seen in MIME (and other) sensors. This drift generally occurs over long time scales and is significant primarily because it limits ones ability to use signal averaging to suppress the effect of the other noise sources. The largest baseline drifts are typically associated with an initial "burn-in" or "drying" period during which drifts in resistance of as much as an order of magnitude can be observed.

Lastly, although sensitivity and noise are the primary measures of sensor performance of interest here, there are other important characteristics such as the sensor selectivity that are typically achieved using sensor arrays and chemometric algorithms. Smaller sensors would allow denser arrays, and this could be advantageous. Beyond this, the sensor size would critically impact the system's size/weight, its power consumption, and its cost, and it can be expected that scaling would yield benefits in all of these areas.

IV. SENSOR-SCALING EXPERIMENTS

At the outset, it is important to state a basic caveat regarding the experiments and their interpretation. Ideally, a study of chemiresistor scaling would compare devices of varying geometry that all have the same bulk and contact conductivities. This is difficult to achieve in practice however for a number of reasons. First, there is appreciable drift in the sensor conductance (of any size sensor) that is associated with the time since deposition, the exposure history, the temperature, and possibly other factors. Second, as indicated earlier, it is difficult to control the film thickness d as deposited by the airbrush technique especially from batch to batch. Such thick-

ness variations could also occur as a result of shadowing by adjacent electrodes or solvent-evaporation effects that would more likely affect narrow-gap devices. Finally, for the square electrodes [Fig. 2(b), where $L \sim W$] and for the very narrow-gap electrodes (where $L \sim d$), fringing currents can undermine the quasi-1-D transport assumption made by the formulas of the previous section. Data interpreted according to these formulas would then manifest deviations that would appear as scale-dependent conductivity variations. Experiments indicate (see below) that the "conductivity" variations that result from all of these sources are relatively small being at most a factor of two or three (apart from the "aging" effects mentioned earlier). Moreover, because these variations are far smaller than the magnitude of the dimensional changes in W and L that we study, it seems reasonable to base conclusion about the MIME sensor-scaling properties on such data. It should be noted that in this paper, we do not study the effect of varying d.

We divide our presentation of the experimental results into two: first, studying the nanocluster-based sensors in purely electrical terms as resistors and then examining them as transductive elements and specifically as chemiresistors. In actual applications, the sensors would of course be packaged, however, in this paper, all electrical testing was performed by directly probing the bonding pads on the sensor chips. The I–V measurements were performed using a Hewlett-Packard 4145B parameter analyzer, and the noise measurements, as discussed in greater detail in [38], were performed using an SR560 Low-Noise Voltage Preamplifier or an SR570 Low-Noise Current Preamplifier coupled to an SR770 FFT Network Analyzer. All measurements were performed at room temperature, which would of course be the standard operating condition.

The first set of experiments we discuss investigates the extent to which nanocluster films act as homogeneous resistors by obeying (2). To this end, in Fig. 3, we plot the resistance times the width (RW) of airbrushed films as a function of L. Data from devices with the three electrode patterns shown in Fig. 2(a)–(c) are included in the plot. Despite significant scatter in the data (presumably for the reasons explained at the start of this section), the curve fits to the data, also plotted in Fig. 3, show that the data are consistent with ohmic behavior. The dashed straight line is that obtained if the sheet conductivity $(\sigma_{\mathrm{f}} d)$ of the films is taken to be 0.5 ns and if it is assumed that there is no contact resistance $(\sigma_{\mathrm{c}} \to \infty)$. The systematic deviations of the data from that line, as the gap is reduced, indicate that there is a significant contribution from contact resistance.[2] Specifically, the solid-line fit to the data gives the RW variation that would result if the contact conductivity $(\sigma_{\mathrm{c}} d)$ was 2.5 ns/μm. Based on these numbers, we deduce that $\beta \cong 0.4 \, \mu\mathrm{m}/L$, meaning that contact effects become significant when $L \sim 0.4 \, \mu\mathrm{m}$ or smaller. In the case of the narrow-gap $(\sim 0.1 \, \mu\mathrm{m})$ devices, Fig. 3 shows that the contact resistance supplies about 75% of the total resistance. That there is an extra contact contribution suggests that the tunneling situations

---

[2]It is conceivable that the deviations in Fig. 3 could be the result of a shadowing effect of the electrodes during the airbrush deposition that results in narrower gap electrodes having thinner films and thus increased resistances.
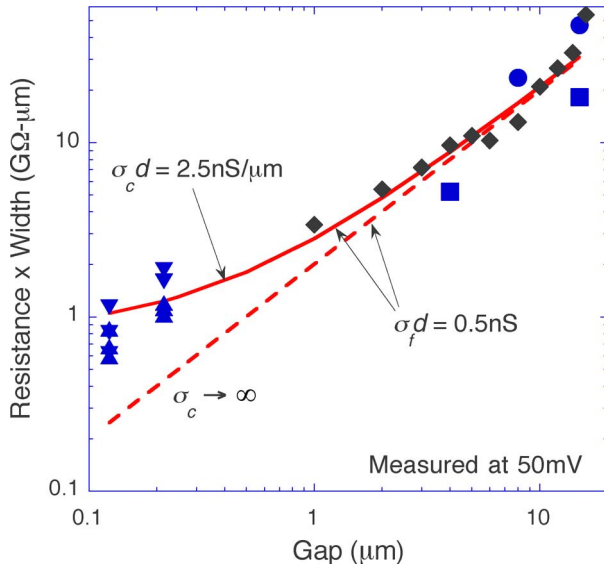
Fig. 3. Log–log plot of the resistance times width (RW) of air-brushed MIME films as a function of the size of the electrode gap (L) over a range from 0.123 to 15 μm. The different symbols correspond to different chips and batches, respectively, with the circles and squares being for interdigitated designs like those of Fig. 2(a), the diamonds being for the electrode design of Fig. 2(b) with $W = 90$ μm, and the triangles being for interdigitated designs like those of Fig. 2(c). The dashed line is a fit assuming ohmic behavior and no contact resistance ($\sigma_c \rightarrow \infty$), whereas the solid curve includes also contact resistance. The scatter in the plot is believed due to the drift in the sample characteristics as discussed in the text.
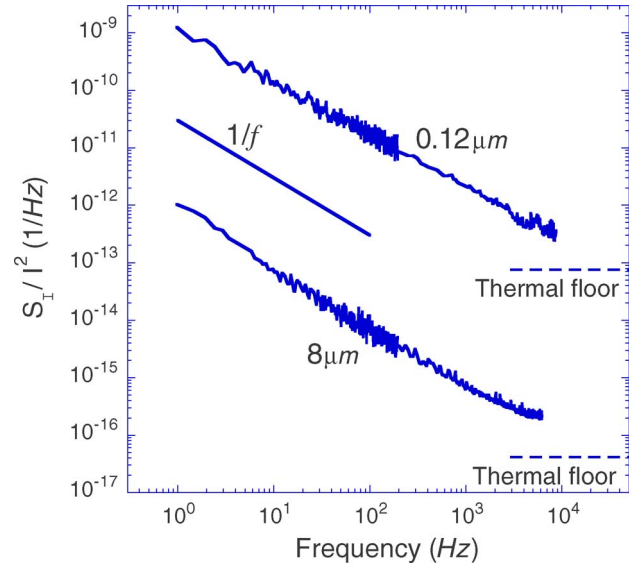

Fig. 4. Current-noise spectral density normalized by the square of the dc current as a function of frequency. At high frequencies, the noise approaches the thermal/system noise floor, while at lower frequencies, $1/f$ noise clearly dominates. The observed increase in the normalized noise spectral density, as a result of scaling, is due to a reduced number of electrons participating in the transport in the smaller sensor.

between the cluster cores of the film and between the electrode and adjacent cluster cores are in fact significantly different.

Next we turn to an examination of the electrical noise in the chemiresistors when no vapor is present. This noise is gauged by the current-noise spectral density S_I that is measured under dc conditions as a function of frequency and voltage. As noted in the Introduction, in this paper, we use the zero-vapor characteristics to judge the noise floor even when vapor is present [37], [38]. Again, understanding the noise is important because it determines how small a vapor-induced resistance change can be detected, which in turn impacts the detection limit of the sensor as discussed in Section V

The frequency dependence of the noise is plotted in Fig. 4 which shows the normalized current-noise spectral density S_I/I^2 as a function of f for chemiresistors of two different sizes (gaps of 8 and 0.12 μm), each having roughly the same W/L. It is evident from the plot that both devices are dominated by flicker noise with a clear $1/f$ dependence extending over nearly four decades in frequency. At the highest frequencies, the curves appear to show the beginnings of a leveling out near their respective thermal noise floors, as calculated from (11) (also shown in Fig. 4) or perhaps at some slightly higher value associated with a system noise floor. (N.B.: The two devices have different thermal and system noise floors because their resistances are different.) From these data, the corner frequency is clearly above 10^4 Hz. Fig. 4 also shows that under constant voltage scaling (for which I will remain fixed), the smaller device has far more noise at a given frequency. Qualitatively, this increase is in accord with the Hooge formula (13b) and is associated with a decline in the number of participating electrons (N) in proportion to the volume of the film. Quan-

titatively, one expects from (13b) that S_I/I^2 should increase by roughly a factor of $(L_{\text{large}}/L_{\text{small}})^2 \cong (8\ \mu\text{m}/0.12\ \mu\text{m})^2 \cong 4400$, and this is in reasonable agreement with the observed increase of about 3000. If one assumes that N is equal to the number of nanoclusters in the films then, based on the data of Fig. 4, the Hooge parameter α_H is estimated to be around ten. This value is considerably larger than those typically seen in semiconductor devices (which are usually around 10^{-4}) and can be ascribed to 1) the fact that the cluster transport is Coulomb blockaded and so involves far fewer conducting electrons and 2) disorder in the system, which is known to increase α_H [38].

The bias dependence of the chemiresistor noise is evident from the fact that the noise characteristics in Fig. 4 are independent of voltage. Thus demonstrates that for these devices, $S_I \sim I^2$ in accord with the Hooge formula (12). To examine the dependence directly, in Fig. 5, we plot S_I as a function of the voltage for two different devices that again had gaps of 8 and 0.12 μm. For both of these devices, when the voltage is appreciable (with $V/L > 100$ V/cm), the noise rises quadratically with bias (i.e., with a slope of two in Fig. 5), again demonstrating agreement with the Hooge formula (13a). At the very lowest voltages/fields, the decline in $1/f$ noise should lead to a leveling out near the thermal noise floors of the two devices, and this is indeed seen at least for the larger device. That the smaller device has more $1/f$ noise at a given voltage is again due to the scaling and the effect of a decreased number of electrons participating in the conduction (N). In the unnormalized noise spectral density of Fig. 5, the scaling effect is moderated somewhat by the contact resistance, as noted in Section III, in relation to (13a). Quantitatively, we expect the factor of 4400 seen earlier but reduced by a resistance factor for these devices of $(R_{\text{small}}/R_{\text{large}})^2 \cong (45.2\ \text{k}\Omega/2.45\ \text{k}\Omega)^2 \cong 340$. Thus, the noise in the smaller device should be amplified by a factor of $4400/340 \sim 13$, which is comparable to the experimental value
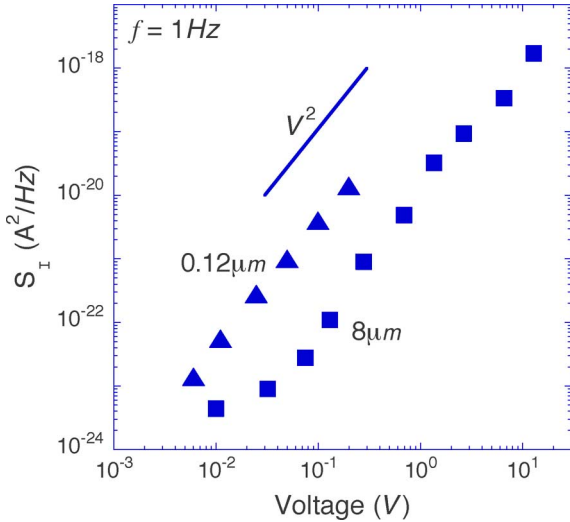
Fig. 5. Current-noise spectral density as a function of voltage. At very low voltages, the noise approaches a thermal/system floor (apparent in the 8-μm device), while at higher biases, the $1/f$ component dominates.
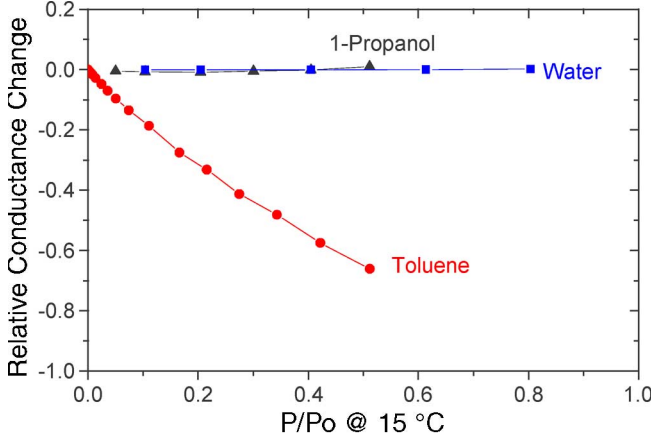

Fig. 6. Relative resistance change of a micrometer-scale MIME sensor as a function of the normalized partial pressures of several analyte vapors. Note that $P/P_o = 0.001$ corresponds to 19 ppmv.

of about 23. Further discussion of the sensor noise, its scaling characteristics, and its effect on the detection limit appears in Section V.

To introduce the subject of the vapor response of MIME sensors, we first review some results for conventional micrometer-scale MIME devices that provide an indication of the operating characteristics and performance of these sensors [7]–[9], [31]. In Fig. 6, we plot the relative resistance changes that result when such a MIME sensor with a film composed of hexanethiol-coated clusters is exposed to varying concentrations of several different test analytes. These curves are essentially linear at lower exposure levels as expected from the discussion in Section III. Based on these data and (9), we can estimate the film's normalized responses as measured by $k_a r_a^f / \sigma_1$ for the various analytes, as shown in Table I. The sign of this quantity is determined by the sign of r_a^f (since the other factors are always positive). Negative values are associated with an increase in resistance resulting from the aforementioned swelling mechanism, while the positive values are believed due to a dipole-induced barrier lowering that

TABLE I
NORMALIZED RESPONSE OF A CHEMIRESISTOR FORMED OF
HEXANETHIOL-COATED CLUSTERS TO VARIOUS ANALYTES
AS ESTIMATED FROM THE DATA IN FIG. 6

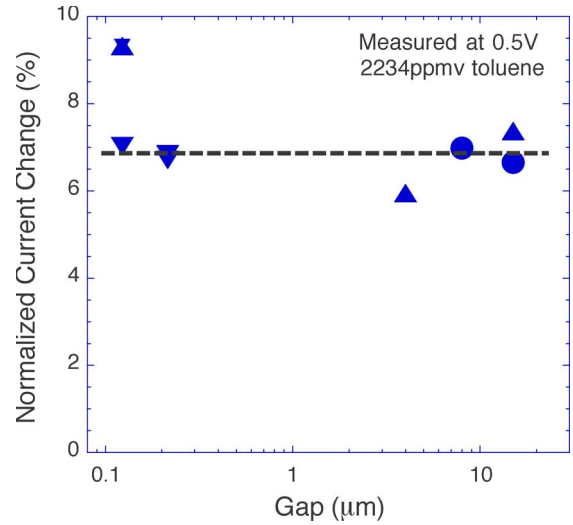|	Toluene	Propanol	Water
$k_a r_a^f / \sigma_l$ (10^{-5}/ppmv)	-11.0	-0.26	~ 0

Fig. 7. Dependence of the relative current change for $V = 0.5$ V induced by a fixed vapor exposure (2234 ppmv of toluene) on the gap distance L for the interdigitated devices of Fig. 2(a)–(c). All of the devices had the same $W/L = 32\,000$, and the different symbols correspond to devices from different batches.

decreases the resistance. The reversal in sign of the response to 1-propanol at relatively low-exposure levels suggests that it is affected by both of these mechanisms. Last, the relative insensitivity of this particular nanocluster film to water is an attractive feature for many applications.

For a first look at the scaling behavior of the vapor response, we examine the dependence of the relative current change ($\Delta I/I$) on geometry. As was discussed in Section III in relation to (8) and (9), the relative current change is of value for interpreting measurements because many of the geometrical dependences of the absolute current change drop out. Consequently, such a plot will afford a perspective on the degree to which ideal chemiresistive behavior is being observed and also on film's intrinsic response. To this end, in Fig. 7, we plot the relative current change induced by an exposure to 2234 ppmv of toluene vapor as functions of the gap L for the devices shown in Fig. 2(a) and (c) that all had the same W/L. The basic qualitative observation from these plots is that the normalized current change is altered very little when L (and W) are changed by over two orders of magnitude. In other words, the data fit (8) quite well if the film and contact chemiresistances are assumed to be roughly identical ($r \cong 1$). That the chemiresistance (Fig. 7) does not manifest clear contact-related deviations like those shown in the resistance (Fig. 3) is somewhat surprising. Last, from Fig. 7 and (9), we can determine that $k_{tol} r_{tol}^f / \sigma_f \cong -7 \times 10^{-5}$/ppmv, a number that is slightly smaller than the value for toluene given in Table I with the difference presumed due to differences in the intrinsic properties of the two films, which were deposited several years
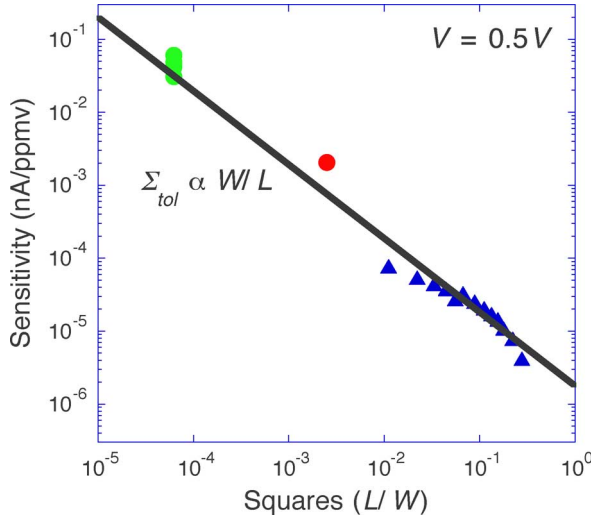
Fig. 8. Plot of the chemiresistor sensitivity as a function of the number of squares in the device. As shown in the figure, the ohmic prediction of an inverse relationship is valid over a wide range. The different symbols correspond to different electrode designs. The circles are for interdigitated designs like those of Fig. 2(a) with L ranging from 4 to 15 μm; the triangles are for the electrode design of Fig. 2(b) with L ranging from 1 to 25 μm; and the circle is for an ultrasmall device with a $W = 10$ μm and $L = 0.025$ μm (not shown in Fig. 2).
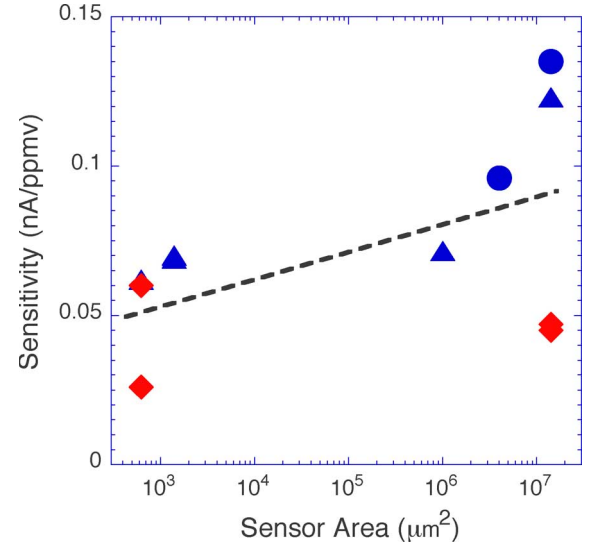

Fig. 9. Plot of the chemiresistor sensitivity as sensor area (the data for the small geometry devices has been scaled up to reflect a 23% difference in the actual W/L). The different symbols correspond to different airbrush batches.

W/L and V constant (Fig. 5). The overall performance degradation that results is discussed in the next section.

apart and to the different vapor handling systems used in the two measurements.

From Fig. 7 we conclude that the MIME sensors behave as macroscopic chemiresistors over the entire range of sizes down to a gap of around 0.1 μm. Moreover, because no contact chemiresistance effect is observed, we can conclude from (6) that the absolute sensitivity of the sensor will increase in proportion to the W/L ratio if V is held constant. Confirming this point, in Fig. 8, we show a plot of Σ_{tol} for a variety of MIME devices of differing dimensions (including one ultrasmall device with $L = 0.025$ μm) as a function of the number of squares (L/W). Clearly, the above formula is accurately obeyed so that the sensor's absolute sensitivity does indeed vary inversely with the number of squares.

Another conclusion that can be reached from (6) is that one can achieve the same sensitivity with a much smaller MIME sensor simply by scaling it in size while keeping W/L and V constant. Experimental data demonstrating that this is true is shown in Fig. 9. In this plot, a small adjustment in the scaled MIME data of 23% has been made to account for these devices having a slightly smaller W/L ratio than the larger devices. Despite the scatter in the data (whose main sources were discussed earlier), it is evident that a change in sensor area by over four orders of magnitude results in a little change in absolute sensitivity. It seems reasonable to conjecture that macroscopic chemiresistor behavior could extend down to gaps as small as 25–50 nm (10–20 clusters). At the extreme, if the required interdigitated electrodes could be made, their total area would be only about 36 μm^2.

That the absolute sensitivity is unchanged by scaling when W/L and V are held constant (Fig. 9) might seem attractive; however, what is important is the signal-to-noise ratio, and, as we have seen, the noise increases during a scaling that keeps

V. DETECTION LIMIT AND OPERATIONAL IMPLICATIONS

In this section we focus on operational questions under the simplifying assumption that our goal, for a given sized sensor, is to optimize the detection limit. Other design tradeoffs such as selectivity, power, and cost that would enter into the engineering of an actual sensor system are ignored.

In general terms, the detection limit is defined as the lowest concentration of analyte that can be reliably detected.[3] Minimizing the detection limit obviously demands that we maximize signal while minimizing noise. To be more quantitative, we define the detection limit c_a^{detlim} for a given sensor as the vapor concentration that will produce a signal-to-noise ratio of one. As in heterodyne receivers (and as has been discussed for chemiresistors in [41]), the best strategy for achieving the minimum detection limit is to operate under ac conditions and use filtering to suppress the low-frequency contribution of the $1/f$ noise. This presumes a sensor system with time constants that, through the use of a preconcentrator, are short enough to allow the vapor exposure to be switched on quickly. To understand and evaluate this strategy, we take the signal to be the rms current change induced by a given vapor exposure and the noise to be the rms noise current. The detection limit is then given by

$$c_a^{\text{detlim}} = \frac{I_{\text{noise}}(\text{rms})}{\Sigma_a(\text{rms})}. \tag{14}$$

---

[3] An alternative terminology for the detection limit is the minimum detectable signal. To be precise, it should also be noted that we here refer to the concentration detection limit; there is also a number detection limit associated with (11) that is defined as the lowest number of analyte molecules that can be reliably detected.

It should be emphasized that this is an "intrinsic" detection limit. The "realizable" detection limit would contain additional multiplicative factors accounting for 1) the noise figure of the measurement amplifier and 2) the actual minimum signal-to-noise ratio, which, depending on the sophistication of one's signal processing, could easily be larger than one.

Although the sensor characteristics described in Section IV were measured under electrically dc conditions, they should provide an accurate representation of the behavior under ac conditions up to the RC cutoff frequency f_{RC} of the sensor that in our devices is roughly 10 kHz. This conclusion is based on the fact that the other electrical time constants of the system, likely associated with charging effects in the insulator and "molecular" responses of the cluster shells, are obviously much shorter than the RC time constant of the entire device. With an applied sinusoidal bias of frequency f, from (7) (which applies since $r \cong 1$, as was noted earlier), the absolute sensitivity will be given by

$$\Sigma_a(\text{rms}) \cong \frac{k_a V_{ac} W d r_a^f}{\sqrt{2} L} \tag{15}$$

where V_{ac} is the amplitude of the applied bias. Similarly, the rms noise current will take the form

$$I_{\text{noise}}(\text{rms}) = \left[\int_{f - \frac{\Delta f}{2}}^{f + \frac{\Delta f}{2}} S_I \, df \right]^{1/2}$$

$$= \sqrt{\frac{k_B T \Delta f}{R} + \frac{\alpha_H V_{ac}^2}{2 N R^2} \ln \left(\frac{f + \frac{\Delta f}{2}}{f - \frac{\Delta f}{2}} \right)} \tag{16}$$

where Δf is the bandwidth of the measurement system, and the second equality assumes the current-noise spectral density to be a sum of the thermal noise (11) and $1/f$ noise (12) components. Combining (14)–(16) then yields

$$c_a^{\text{detlim}} = \frac{\sqrt{2} L}{k_a V_{ac} W d r_a^f} \sqrt{\frac{k_B T \Delta f}{R} + \frac{\alpha_H V_{ac}^2}{2 N R^2} \ln \left(\frac{f + \frac{\Delta f}{2}}{f - \frac{\Delta f}{2}} \right)}. \tag{17}$$

According to (17), if the amplitude of the applied bias were small enough and/or the operating frequency were sufficiently high, thermal noise (i.e., the first term in the square root) would determine the detection limit. In this regime, (17) dictates that the detection limit would be independent of frequency, and one could improve the detection limit by raising the voltage (V_{ac}). However, this procedure would quickly saturate as the $1/f$-noise contribution (i.e., the second term in the square root) grew in size, as in Fig. 5. The asymptotic value that would be reached—thereby defining the **minimum detection limit**—is readily found by neglecting the thermal noise term in (17) to obtain

$$c_a^{\text{min}} = \frac{\sigma_f}{k_a r_a^f (1 + \beta)} \sqrt{\frac{\alpha_H}{N} \ln \left(\frac{f + \frac{\Delta f}{2}}{f - \frac{\Delta f}{2}} \right)}. \tag{18}$$
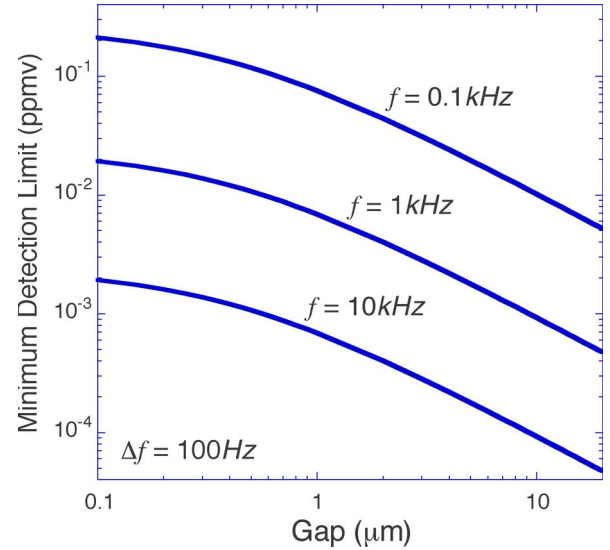

Fig. 10. Illustrative calculation of the minimum detection limits of nanocluster-based chemiresistors as functions of the gap distance L and with the operating frequency as a parameter. The limit degrades as the gap decreases with the roll-off for very narrow gaps being due to contact effects.

This minimum detection limit is nearly always attainable since it is generally achieved at electric fields below 10^4 V/cm.[4] The fact that c_a^{min} decreases with frequency restates the obvious that, to achieve the best sensor performance, one should operate at high frequency as possible (below f_{RC}) and with a measurement system having as narrow bandwidth as possible (like that provided by a lock-in amplifier) so as to minimize the effect of $1/f$ noise. Most importantly, in this paper, the minimum detection-limit scales in inverse proportion to $\sqrt{N} \sim \sqrt{WLd} = L\sqrt{Wd/L}$, at least for larger devices. Assuming d and W/L are held fixed, the latter equality indicates that the minimum detection limit will degrade as L is scaled down. This behavior is illustrated in Fig. 10, where we plot the minimum detection limit as a function of gap L for several different frequencies and assuming $W/L = 32\,000$, and $\Delta f = 100$ Hz. Interestingly, for very small devices, the degradation moderates as the effect of contact resistance becomes important via the factor β. Although this plot is meant primarily to highlight trends, it suggests that under optimum conditions, detection limits below 1 parts-per-billion by volume may be reachable with a conventional micrometer-scale device.

VI. CONCLUSION

The effect of geometric scaling on the performance of gold nanocluster-based MIME sensors has been investigated. Because of the ultrasmall size of the nanoclusters, these sensors

---

[4]As noted in the Introduction, had this minimum detection limit been voltage-dependent, then it would be important to distinguish between constant-voltage and constant-field scaling, with some preference being given to the latter. As it is, however, the distinction is unimportant: In constant-voltage scaling, the sensitivity is independent of size (Fig. 9) and the noise worsens (Fig. 5), while in constant-field scaling, the sensitivity degrades, but the noise stays the same so that, in both cases, the same performance degradation results, as given by (18).

can be scaled by over four orders of magnitude in area and still exhibit essentially the same absolute sensitivity. This behavior appears to be maintained despite a growing contribution of the contacts to the overall resistance of the chemiresistor. However, because of a rising level of $1/f$ noise, the detection limit degrades with scaling. This effect can be mitigated somewhat by operating at high frequency as possible below the device cutoff frequency and with appropriate narrowband filtering. Nevertheless, there is a penalty to be paid for reducing the size of the MIME sensor, and in the design of a nanocluster-based sensing system, this loss in performance needs to be traded off against scaling benefits such as substantial reductions in system size, power requirements, complexity, and cost. It is also possible that extreme scaling of the sensors could open up new application possibilities, e.g., for sensor arrays.

REFERENCES

[1] C. D. Keating and D. L. Feldheim, "Self-assembly of single-electron transistors and related devices," *Chem. Soc. Rev.*, vol. 27, no. 1, pp. 1–12, Jan. 1998.

[2] J. Kong, N. R. Franklin, C. W. Zhou, M. B. Champline, S. Peng, K. J. Cho, and H. J. Dai, "Nanotube molecular wires as chemical sensors," *Science*, vol. 287, pp. 622–625, Jan. 2000.

[3] L. Valentini, I. Armentano, J. M. Kenny, C. Cantalini, L. Lozzi, and S. Santucci, "Sensors for sub-ppm NO2 gas detection based on carbon nanotube thin films," *Appl. Phys. Lett.*, vol. 82, no. 6, pp. 961–963, Feb. 2003.

[4] Q. F. Pengfei, O. Vermesh, M. Grecu, A. Javey, O. Wang, H. J. Dai, S. Peng, and K. J. Cho, "Toward large arrays of multiplex functionalized carbon nanotube sensors for highly sensitive and selective molecular detection," *Nano Lett.*, vol. 3, no. 3, pp. 347–351, Mar. 2003.

[5] J. Li, Y. J. Lu, Q. Ye, M. Cinke, J. Han, and M. Meyyappan, "Carbon nanotube sensors for gas and organic vapor detection," *Nano Lett.*, vol. 3, no. 7, pp. 929–933, Jul. 2003.

[6] J. P. Novak, E. S. Snow, E. J. Houser, D. Park, J. L. Stepnowski, and R. A. McGill, "Nerve agent detection using networks of single-walled carbon nanotubes," *Appl. Phys. Lett.*, vol. 83, no. 19, pp. 4026–4028, Nov. 2003.

[7] A. W. Snow and H. Wohltjen, "Size-induced metal to semiconductor transition in a stabilized gold cluster ensemble," *Chem. Mater.*, vol. 10, no. 4, pp. 947–949, Apr. 1998.

[8] H. Wohltjen and A. W. Snow, "Colloidal metal-insulator-metal ensemble chemiresistor sensor," *Anal. Chem.*, vol. 70, no. 14, pp. 2856–2859, Jul. 1998.

[9] H. Wohltjen and A. W. Snow, "Materials, method and apparatus for detection and monitoring of chemical species," U.S. Patent 6 221 673, Apr. 24, 2001. Subsequent work is contained in proprietary reports of Microsensor Systems, Inc.

[10] Y. Joseph, B. Guse, A. Yasuda, and T. Vossmeyer, "Chemiresistor coatings from Pt- and Au- nanoparticle/nonanedithiol films: Sensitivity to gases and solvent vapors," *Sens. Actuators B, Chem.*, vol. 98, no. 2/3, pp. 188–195, Mar. 2004.

[11] H. Wohltjen, W. R. Barger, A. W. Snow, and N. L. Jarvis, "A vapor-sensitive chemiresistor fabricated with planar microelectrodes and a Langmuir-Blodgett organic semiconductor film," *IEEE Trans. Electron Devices*, vol. ED-32, no. 7, pp. 1170–1174, Jul. 1985.

[12] N. R. Byrd, "Space cabin atmosphere containment measurement techniques," NASA Electron. Res. Center, Cambridge, MA, Rep. SM-48446-F, Jul. 1968. Contract NAS12-15, NASA CR-86047, DTIC ADB217286.

[13] B. Rosenber, T. N. Misra, and R. Switzer, "Mechanism of olfactory transduction," *Nature*, vol. 217, no. 5127, pp. 423–427, Feb. 1968.

[14] J. Kaufhold and K. Hauffe, "Uber das leitfahigkeitsverhalten verschieder phthalocyanine im vakuum und unter dem einflais von gasen," *Ber. Bunsen-Gessel. Physik. Chemie*, vol. 69, no. 2, p. 168, 1965.

[15] H. E. Katz, "Chemically sensitive field-effect transistors and chemiresistors: New materials and device structures," *Electroanalysis*, vol. 16, no. 22, pp. 1837–1842, Nov. 2004.

[16] J. Janata, "Electrochemical microsensors," *Proc. IEEE*, vol. 91, no. 6, pp. 864–869, Jun. 2003.

[17] R. A. Bailey and K. C. Persaud, *Polymer Sensors and Actuators*, Y. Osata and D. E. DeRossi, Eds. Berlin, Germany: Springer-Verlag, 2000, ch. 5.

[18] J. Janata, M. Josowicz, P. Vanysek, and D. M. DeVaney, "Chemical Sensors," *Anal. Chem.*, vol. 70, no. 12, pp. 179R–208R, Jun. 1998.

[19] A. W. Snow and W. R. Barger, *Phthalocyanines: Properties and Applications*, vol. 1, C. C. Leznoff and A. B. P. Lever, Eds. New York: VCH, 1989, ch. 5.

[20] J. Janata and A. Bezegh, "Chemical sensors," *Anal. Chem.*, vol. 60, no. 12, pp. R62–R74, Jun. 1988.

[21] J. P. Dolan and W. M. Jordan, U.S. Patent 3 045 198, Jul. 17, 1962.

[22] B. Lundberg and B. Sundqvist, "Resistivity of a composite conducting polymer as a function of temperature, pressure and environment—Applications as a pressure and gas concentration transducer," *J. Appl. Phys.*, vol. 60, no. 3, pp. 1074–1079, Aug. 1986.

[23] G. R. Ruschau, R. E. Newnham, J. Runt, and B. E. Smith, "0–3 ceramic polymer composite chemical sensors," *Sens. Actuators*, vol. 20, no. 3, pp. 269–275, Dec. 1989.

[24] P. Talik, M. Zabdowska-Waclawek, and W. Waclawek, "Sensing properties of the CB-PCV composites for chlorinated-hydrocarbon vapors," *J. Mater. Sci.*, vol. 27, no. 24, pp. 6807–6810, Dec. 1992.

[25] M. C. Lonergan, E. J. Severin, B. J. Doleman, S. A. Beaber, R. H. Grubb, and N. S. Lewis, "Array-based vapor sensing using chemically sensitive, carbon back-polymer resistors," *Chem. Mater.*, vol. 8, no. 9, pp. 2298–2312, Sep. 1996.

[26] J. Li. (2000). *Sensors Online Magazine*, vol. 17. [Online]. Available: http://www.sensorsmag.com/articles/0800/56/main.shtml

[27] J. W. Gardner, Z. Iskandarani, and B. Bott, "Effect of electrode geometry on gas sensitivity of lead phthalocyanine thin films," *Sens. Actuators B, Chem.*, vol. 9, no. 2, pp. 133–142, Aug. 1992.

[28] P. Ingleby, J. W. Gardner, and P. N. Bartlett, "Effect of micro-electrode geometry on response of thin-film poly(pyrrole) and poly(aniline) chemiresistive sensors," *Sens. Actuators B, Chem.*, vol. 57, no. 1–3, pp. 17–27, Sep. 1999.

[29] B. Mathews, J. Li, S. Sunshine, L. Lerner, and J. W. Judy, "Effects of electrode configuration on polymer carbon-black composite chemical vapor sensor performance," *IEEE Sensors J.*, vol. 2, no. 6, pp. 160–168, Jun. 2002.

[30] M. Brust, M. Walker, D. Bethell, D. J. Shiffrin, and R. Whyman, "Synthesis of thiol-derivatized gold nanoparticles in a 2-phase liquid–liquid system," *J. Chem. Soc.—Chem. Commun.*, vol. 7, pp. 801–802, Apr. 1994.

[31] A. W. Snow, H. Wohltjen, and N. L. Jarvis, *2002 NRL Review*, pp. 45–55, 2002. [Online]. Available: http://www.nrl.navy.mil/content.php?P=02REVIEW45

[32] M. E. Franke, T. J. Koplin, and U. Simon. (2006). Metal and metal oxide nanoparticles in chemiresistors: Does the nanoscale matter? *Small*, pp. 36–50. [Online]. *2(1)* Available: www.small-journal.com

[33] L. Mingtao, L. Chen, Z. Wei, and S. Y. Chou, "Pattern transfer fidelity of nanoimprint lithography on six-inch wafers," *Nanotechnology*, vol. 14, no. 1, pp. 33–36, Jan. 2003.

[34] A. W. Snow, M. G. Ancona, W. Kruppa, G. G. Jernigan, E. E. Foos, and D. Park, "Self-assembly of gold nanoclusters on micro- and nanoelectronic substrates," *J. Mater. Chem.*, vol. 12, no. 4, pp. 1222–1230, 2002.

[35] V. Santhanam and R. P. Andres, "Microcontact printing of uniform nanoparticle arrays," *Nano Lett.*, vol. 4, no. 1, pp. 41–44, Jan. 2004.

[36] R. M. van Dam, S. R. Quake, A. Scherer, and M. O. Reese, "Micro fabricated fountain pen apparatus and method for ultra high density biological arrays," U.S. Patent 0 148 539, Aug. 7, 2003.

[37] C. Kurdak, J. Kim, A. Kuo, J. J. Lucido, L. A. Farina, X. Bai, M. P. Rowe, and A. J. Matzger, "1/f noise in gold nanoparticle chemosensors," *Appl. Phys. Lett.*, vol. 86, no. 7, p. 073506, Feb. 2005.

[38] W. Kruppa, M. G. Ancona, R. W. Rendell, A. W. Snow, E. E. Foos, and R. Bass, "Electrical noise in gold nanocluster sensors," *Appl. Phys. Lett.*, vol. 88, no. 5, p. 053120, Feb. 2006.

[39] J. Sikula, M. Levinshtein, Eds. *Advanced Experimental Methods for Noise Research in Nanoscale Electronic Devices*, vol. 151, Dordrecht, The Netherlands: Kluwer, 2004.

[40] F. N. Hooge, "1/f noise is no surface effect," *Phys. Letts. A*, vol. 29, no. 3, p. 139, Apr. 1969.

[41] H. V. Shurmer, P. Corcoran, and M. K. Jones, "Sensitivity enhancement for gas-sensing and electronic nose applications," *Sens. Actuators B, Chem.*, vol. 16, no. 1–3, pp. 256–259, Oct. 1993.

Mario G. Ancona received the B.E.S. degree from Johns Hopkins University, Baltimore, MD, in 1976 and the Ph.D. degree from Rensselaer Polytechnic Institute, Troy, NY, in 1980.

He is currently a Research Physicist with the Naval Research Laboratory, Washington, DC, working in the areas of semiconductor devices, sensors, and nanoelectronics.

Arthur W. Snow received the B.S. degree in chemistry from Michigan State University (MSU), East Lansing, and the Ph.D. degree in polymer chemistry from the City University of New York, in 1971 and 1977, respectively.

After graduating from MSU, he rendered brief military service. After a year at the American Cyanamid Company, he joined the Naval Research Laboratory (NRL), Washington, DC, as a National Research Council Research Associate, in 1978, and became an NRL staff member as a Research Chemist in 1979. His research interests are polymer synthesis, electroactive polymers, low-dielectric polymers, chemical microsensors, metal nanoclusters, and nonlinear optical materials.

Edward E. Foos received the B.S. degree in chemistry from Miami University, Oxford, OH, in 1944 and the Ph.D. degree in chemistry from Duke University, Durham, NC, in 1998.

He is currently a Research Chemist at the U.S. Naval Research Laboratory, Washington, DC, studying the synthesis and self-assembly of metal and semiconductor nanoparticles.

Walter Kruppa (M'84–SM'00) received the B.S. degree in electrical engineering (with distinction) from the University of Akron, Akron, OH, in 1962. He received the M.S. and Ph.D. degrees in electrical engineering from The Ohio State University, Columbus, in 1963 and 1969, respectively, with fellowships from the Bell Telephone Laboratories.

He then took a position with Bell Telephone Laboratories, and his work consisted of developing various microwave components including traveling-wave tubes, parametric amplifiers, GaAs field-effect transistors, and high-speed integrated circuits for use in coaxial and fiber-optic transmission systems. In 1982, he joined George Mason University, Fairfax, VA, as an Associate Professor of electrical engineering. He took his current position with the Naval Research Laboratory, Washington, DC, in 1996. His research interests are in the areas of InAs- and GaN-channel HEMTs, high-speed analog and digital circuits, and nanoelectronic devices.

Robert Bass received the B.S. degree in physics from Drexel Institute of Technology, Philadelphia, PA, in 1996, and the M.S. and Ph.D. degrees in physics from Michigan State University, East Lansing, in 1968 and 1972, respectively.

During the next 17 years, he pursued a career in the teaching profession holding positions at the University of Mississippi, Oxford, Concord High School, Wilmington, DE, and Prince George's Community College, Largo, MD. In 1989, he joined the Nanoelectronics Processing Facility at the Naval Research Laboratory (NRL), Washington, DC, as a Research Physicist in the area of electron beam lithography. He has been a Principle Investigator for the Defense Advanced Research Projects Agency's (DARPA's) Advanced Lithography Program and has provided lithographic expertise to universities and other government agencies requiring nanolithography. He is currently providing electron beam lithography support and process development for various projects at NRL including III-V HEMT development, chemical, and biological sensors.